THE JOURNAL OF BIOLOGICAL CHEMISTRY VOL. 287, NO. 52, pp. 43351–43358, December 21, 2012

The Mammalian Proteins MMS19, MIP18, and ANT2 Are Involved in Cytoplasmic Iron-Sulfur Cluster Protein Assembly*[S]

Received for publication, October 26, 2012, and in revised form, November 13, 2012 Published, JBC Papers in Press, November 13, 2012, DOI 10.1074/jbc.M112.431270

Niek van Wietmarschen[‡], Annie Moradian[§], Gregg B. Morin[§¶], Peter M. Lansdorp[‡‖1], and Evert-Jan Uringa[‡‖2]**

*From the [‡]European Research Institute for the Biology of Ageing, University Medical Center Groningen, University of Groningen, Antonius Deusinglaan 1, 9713 AV Groningen, The Netherlands, the [§]Michael Smith Genome Sciences Centre, British Columbia Cancer Agency, Vancouver, British Columbia V5Z 4E6, Canada, the [¶]Department of Medical Genetics, University of British Columbia, Vancouver, British Columbia V5Z 4E3, Canada, the [‖]Terry Fox Laboratory, British Columbia Cancer Agency, Vancouver, British Columbia V5Z 1L3, Canada, and the **Division of Hematology, Department of Medicine, University of British Columbia, Vancouver, British Columbia V5Z 4E3, Canada*

Background: MMS19 was recently identified as part of the cytosolic iron-sulfur (Fe-S) cluster assembly (CIA) machinery.
Results: MMS19 and MIP18 both interact with CIA and Fe-S proteins, and ANT2 binds to this complex.
Conclusion: MMS19, MIP18, and ANT2 facilitate Fe-S cluster insertion into cytosolic Fe-S proteins.
Significance: Identification of proteins in the CIA complex elucidates aspects of cytoplasmic iron-sulfur cluster assembly.

Iron-sulfur (Fe-S) clusters are essential cofactors of proteins with a wide range of biological functions. A dedicated cytosolic Fe-S cluster assembly (CIA) system is required to assemble Fe-S clusters into cytosolic and nuclear proteins. Here, we show that the mammalian nucleotide excision repair protein homolog MMS19 can simultaneously bind probable cytosolic iron-sulfur protein assembly protein CIAO1 and Fe-S proteins, confirming that MMS19 is a central protein of the CIA machinery that brings Fe-S cluster donor proteins and the receiving apoproteins into proximity. In addition, we show that mitotic spindle-associated MMXD complex subunit MIP18 also interacts with both CIAO1 and Fe-S proteins. Specifically, it binds the Fe-S cluster coordinating regions in Fe-S proteins. Furthermore, we show that ADP/ATP translocase 2 (ANT2) interacts with Fe-S apoproteins and MMS19 in the CIA complex but not with the individual proteins. Together, these results elucidate the composition and interactions within the late CIA complex.

Fe-S clusters are inorganic cofactors of proteins functioning in many cellular processes including DNA metabolism, transcription, translation, electron transport, oxidative phosphorylation, and cellular metabolism. Fe-S clusters themselves are relatively simple structures, consisting of several iron cations (Fe^{2+} or Fe^{3+}) and sulfur anions (S^{2-}) (1). However, their assembly into proteins within a cell is a complex process, for which many different proteins are required. In eukaryotes, Fe-S clusters are assembled at two different sites by two different systems. Mitochondrial Fe-S proteins receive their Fe-S clusters from the mitochondrial Fe-S cluster (ISC)[3] assembly system, which comprises components that are very similar to those found in the bacterial ISC system. The first step for assembly of Fe-S clusters into cytosolic and nuclear Fe-S proteins requires the ISC system, after which an iron compound is exported from the mitochondria. The Fe-S cluster is subsequently further processed by the cytosolic iron-sulfur cluster assembly (CIA) machinery, after which the clusters are incorporated into their target proteins (2). Both the ISC and CIA systems are highly conserved in eukaryotes, from yeast to human, pointing to the crucial importance of proper Fe-S cluster assembly (3).

In the yeast CIA system, Fe-S clusters are transiently assembled on the scaffold proteins cytosolic Fe-S cluster assembly factors NBP35 (Nbp35) and CFD1 (Cfd1) (4, 5) in a step that requires Fe-S cluster assembly protein DRE2 (Dre2) (6). Subsequently, the labile Fe-S cluster is transferred to a complex of two proteins: cytosolic Fe-S cluster assembly factor NAR1 (Nar1) (7) and the WD40-repeat protein, cytosolic Fe-S assembly protein 1 (Cia1). Finally, Fe-S clusters are transferred to and incorporated in target proteins (8).

Mammalian homologs of Cia1 (CIAO1), Dre2 (anamorsin, CIAPIN1), Nar1 (cytosolic Fe-S cluster assembly factor NARFL), Nbp35 (cytosolic Fe-S cluster assembly factor NUBP1), and Cfd1 (cytosolic Fe-S cluster assembly factor NUBP2) have been identified as components of the CIA system in mammals (3). Until recently, little was known about how Fe-S clusters are transferred from the CIAO1-NARFL complex to target Fe-S proteins, as no direct interaction between Fe-S cluster donor and acceptor proteins had been shown. However, two recent studies report that MMS19 is in complex with several Fe-S proteins and the CIA pro-

* This work was supported by Grant 018006 awarded by the Terry Fox Foundation Program Project and Grant 105265 from the Canadian Cancer Society.
[S] This article contains supplemental Tables S1 and S2.
[1] To whom correspondence may be addressed: European Research Inst. for the Biology of Ageing, University Medical Centre Groningen, Antonius Deusinglaan 1, 9713 AV Groningen, The Netherlands. E-mail: p.m.lansdorp@umcg.nl.
[2] To whom correspondence may be addressed: European Research Inst. for the Biology of Ageing, University Medical Centre Groningen, Antonius Deusinglaan 1, 9713 AV Groningen, The Netherlands. E-mail: e.j.uringa@umcg.nl.

[3] The abbreviations used are: ISC, iron-sulfur cluster; IP, immunoprecipitation; CIA, cytosolic iron-sulfur cluster assembly.

teins CIAO1, MIP18 (9, 10), and NARFL (9). Furthermore, in the absence of MMS19, the stability and incorporation of iron into Fe-S proteins is reduced, suggesting that MMS19 is an important factor in the assembly of cytosolic Fe-S cluster proteins (9, 10).

Here we show that MMS19 simultaneously interacts with the CIA protein CIAO1 and the Fe-S cluster target proteins. In addition, we identify the MMS19 region that mediates the interaction with Fe-S proteins. We show that MIP18 is also capable of binding directly to both CIAO1 and Fe-S proteins and that it binds to the Fe-S cluster coordinating regions of Fe-S target proteins. We also found that ANT2 can interact with MMS19 and Fe-S proteins but only in complex, not with the individual proteins. Based on these findings, we propose that MMS19 and MIP18 bridge the gap between Fe-S cluster donor and acceptor proteins. Specifically, we suggest that MMS19 brings Fe-S cluster donor and acceptor proteins into close proximity and that the Fe-S cluster is transferred into the target protein with the help of MIP18. Furthermore, we propose that ANT2 is required to stabilize the interaction between MMS19 and Fe-S proteins.

EXPERIMENTAL PROCEDURES

Cell Lines—HEK293 cells were transfected with a Venus-Myc cDNA fusion construct containing MMS19, CIAO1, or MIP18 mouse cDNA using FuGENE HD (Promega) and selected 36 h after transfection with 3 μg/ml puromycin (Invitrogen). *Rtel1-FLAG* knock-in mouse embryonic stem (ES) cells were grown as described previously (11).

Confocal Microscopy—MMS19-Venus-Myc-expressing HEK293 cells were plated in No. 1.5 Labtek II chambered coverglasses (Nalgene Nunc). Confocal microscopy was performed using an LSM 780 and an iLCI Plan-Neofluar 63x/1.3 oil objective (Zeiss).

Vector Construction—Protein expression vectors were created using the pF25A ICE T7 Flexi vector (Promega) as a backbone. AscI and FseI restriction sites and sequences encoding a 2xMyc tag or 3xFLAG tag were ligated into the vector. Herculase II fusion DNA polymerase (Agilent Technologies) was used to PCR amplify murine cDNA flanked by AscI/FseI sites. PCR products were digested and ligated into the AscI/FseI sites of pF25A ICE T7 2xMyc or 3xFLAG vectors. The cDNAs and oligos used are listed in supplemental Table S1.

In Vitro Transcription and Translation and Immunoprecipitation (IP)—FLAG- and Myc-tagged proteins were synthesized *in vitro* using the TnT T7 insect cell extract protein expression system (Promega). Proteins were incubated in IP buffer (25 mM HEPES, 1 mM EDTA, 0.1% v/v Nonidet P-40, 150 mM NaCl, and Complete EDTA-free protease inhibitor cocktail (Roche Applied Science)), and IP was performed using anti-FLAG M2-agarose (Sigma-Aldrich, A2220) or anti-c-Myc-agarose (Sigma-Aldrich, A7470). Mock IPs were performed by incubating FLAG-tagged protein with anti-c-Myc-agarose in the absence of Myc-tagged proteins. SDS-PAGE was performed to separate proteins for immunoblot analysis.

Antibodies and Immunoblot Analysis—Antibodies used for immunoblotting are mouse anti-FLAG M2 (Sigma-Aldrich, F1804), rabbit anti-Myc (Abcam, ab9106), mouse anti-MMS19 (Euromedex, MMS-3H10), rabbit anti-Ciao1 (Santa Cruz Biotechnology, sc-8322), rabbit anti-MIP18 (Abcam, ab103227), mouse anti-XPD (Abcam, ab54676), rabbit anti-FANCJ (Abcam, ab7288), rabbit anit-DNA2 (Abcam, ab96488), mouse anti-MPG (Abcam, ab55461), mouse anti-SDHB (Abcam, ab14714), mouse anti-UQCRFS1 (Abcam, ab14746), mouse anti-α-tubulin (Cell Signaling Technology, DM12A), mouse anti-histone H3 (Cell Signaling Technology, 96C19), mouse OXPHOS antibody mixture (Abcam, ab110411), goat anti-mouse IgG-perodixase (Sigma-Aldrich, A5278), and goat anti-rabbit IgG-perodixase (Sigma-Aldrich, A6154). After immunoblotting, blots were treated with SuperSignal West Pico or Femto chemiluminescent substrate (Pierce) before exposing and developing films.

IP and Mass Spectrometry—Nuclear and cytosolic fractions were prepared from MMS19-, CIAO1-, or MIP18-Venus-Myc-expressing HEK293 cells and *Rtel1-FLAG* knock-in murine ES cells using a nuclei isolation kit (Sigma, NUC101), and mitochondria were purified using a mitochondria isolation kit (Abcam, ab110170). Cytoplasmic fractions were diluted using cytoplasmic IP buffer (50 mM Tris-HCl (pH 7.4), 150 mM NaCl, 10% v/v glycerol, 0.2% v/v Triton X-100, 25 mM Hepes, 2 mM EDTA, and protease inhibitors). Nuclei and mitochondria were lysed in nuclear lysis buffer (50 mM Tris-HCl (pH 7.4), 500 mM NaCl, 10% v/v glycerol, 0.5% v/v Triton X-100, 25 mM Hepes, 2 mM EDTA, 5 mM $MgCl_2$, DNaseI (Roche Applied Science), and protease inhibitors). Upon lysis an equal volume of nuclear lysis buffer without NaCl and Triton X-100 was added. The MMS19-, CIAO1-, and MIP18-Venus-Myc protein complexes were immunoprecipitated overnight at 4 °C with anti-c-Myc-agarose (Sigma-Aldrich, A7470). MMS19 protein complexes were immunoprecipitated using MMS19 antibody (EuroMedex, MMS-3H10) immobilized on protein G-agarose (Pierce, 20398). Mock IPs were performed by incubating lysates from untransfected HEK293 cells with mouse IgG or anti-c-Myc-agarose. For Western blot analysis the precipitated proteins were eluted in Laemmli buffer for SDS-PAGE. For mass spectrometry (MS) analysis, the proteins were eluted with 0.5 M formic acid (pH 2) twice for 10 min. The eluates were separated by SDS-PAGE using a 4–12% v/v gradient NuPAGE (Invitrogen). Each lane was excised and divided into 16 pieces, and peptides were prepared for MS analysis as described (12). Peptides were analyzed by HPLC-electrospray-tandem mass spectrometry (MS/MS) on a 4000 QTrap mass spectrometer (Applied Biosystems/Sciex) as described (12). The MS/MS spectra were queried against the SwissProt/UniProt human database (version 57.1) using the Mascot search algorithm (version 2.3.01, Matrix Science). Search parameters were 0.3 and 0.4 Da for precursor and product ion mass tolerance, respectively. Candidate interacting proteins were those present in at least two experimental samples with two or more peptides, having a Mascot score of >50, and not present in the appropriate control samples.

RESULTS

MMS19 and MIP18 Are Part of a Late CIA Complex—Despite the proposed nuclear functions of MMS19 this protein is expressed at higher levels in the cytoplasm than in the nucleus (13). Using cell fractionation and IP, we confirmed that endog-

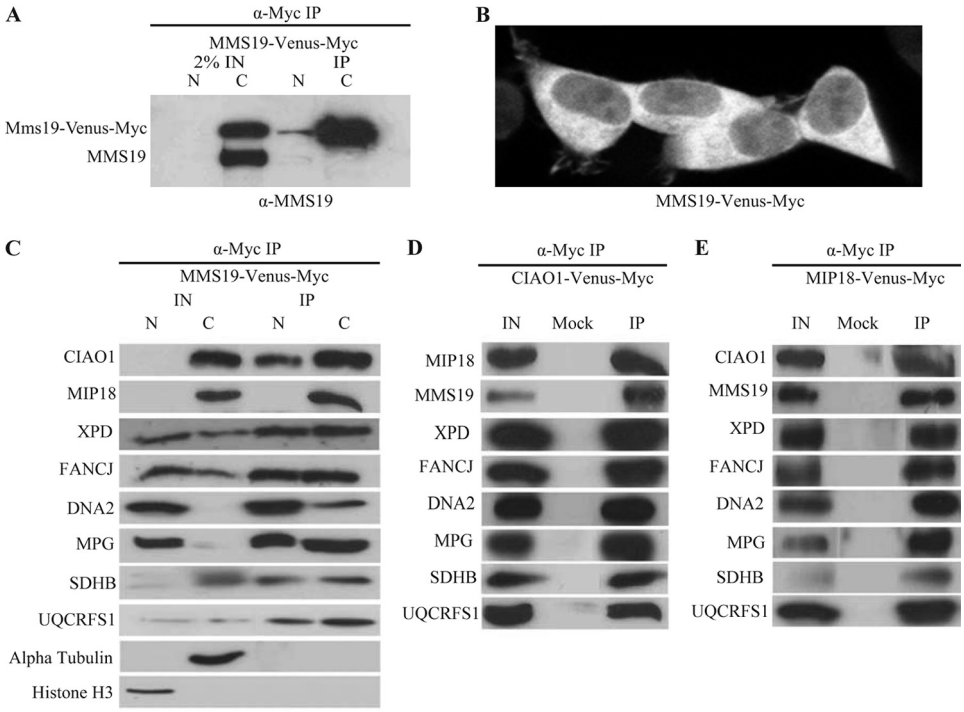

FIGURE 1. **MMS19 and MIP18 are part of a late acting CIA complex.** *A*, anti-MMS19 immunoblot of HEK293 cells expressing MMS19-Venus-Myc. Nuclear and cytoplasmic cell fractions were used for anti-Myc immunoprecipitation. *B*, live cell fluorescent imaging of MMS19-Venus-Myc expressed in HEK293 cells using confocal microscopy. *C–E*, MMS19-Venus-Myc (*C*), CIAO1-Venus-Myc (*D*), or MIP18-Venus-Myc (*E*) were immunoprecipitated from HEK293 cell lysates. Membranes were immunoblotted with the indicated antibodies. The purity of the nuclear and cytosolic fractions was demonstrated by immunoblot detection of histone H3 and α-tubulin, respectively. *N*, nuclear fraction; *C*, cytosolic fraction; *IN*, input; *Mock*, immunoprecipitated fraction; *IP*, immunoprecipitated fraction.

enous MMS19 expression is mainly cytoplasmic (Fig. 1*A*). In addition, epitope- and fluorescently tagged MMS19 (MMS19-Venus-Myc) also localized predominantly to the cytoplasm, as shown by immunoblot detection (Fig. 1*A*) and live cell imaging (Fig. 1*B*). Because tagged-MMS19 showed the same subcellular localization as endogenous MMS19, we used cells expressing tagged MMS19 for further studies. To determine a possible cytoplasmic function of MMS19 we identified cytoplasmic MMS19-interacting proteins. MMS19 and MMS19-Venus-Myc were immunoprecipitated, and complexes were subsequently analyzed using mass spectrometry (supplemental Table S2). CIA complex member CIAO1 was repeatedly found as a potential MMS19-interacting protein as well as MMXD (MMS19-MIP18-XPD) complex members MIP18 and ANT2 (13). Immunoprecipitation of CIAO1 and subsequent mass spectrometry analysis confirmed that MMS19, CIAO1, MIP18, and ANT2 are in the same complex (supplemental Table S2). Mass spectrometry analysis of MMS19-interacting proteins also identified several previously reported Fe-S cluster-containing proteins including NADH dehydrogenase ubiquinone Fe-S protein 1 (NDUFS1), CDK5 regulatory subunit-associated protein 1-like 1 (CDKAL1), t-RNA wybutosine-synthesizing protein 1 homolog (TYW1), phosphoribosylpyrophosphate amidotransferase (PPAT), and Elongator complex protein 3 (ELP3) (supplemental Table S2). These results suggest that MMS19 interacts broadly with Fe-S proteins. This notion is in agreement with mass spectrometry analysis of protein complexes of the Fe-S protein, regulator of telomere length 1 (RTEL1), which also identified MMS19, CIAO1, and MIP18 as potential interacting proteins (supplemental Table S2).

To confirm that MMS19, CIAO1, and MIP18 are part of the same cytosolic complex and that this complex also includes Fe-S proteins, the Myc-tagged proteins were immunoprecipitated from HEK293 cell lysates. Subsequent immunoblotting for MMS19, CIAO1, MIP18, and the Fe-S proteins TFIIH basal transcription factor complex helicase XPD subunit (XPD), Fanconi anemia group J protein (FANCJ), DNA2-like helicase (DNA2), and DNA-3-methyladenine glycosylase (MPG) showed that these proteins were indeed enriched by IP (Fig. 1, *C–E*). These results are in agreement with two recent papers reporting a role for MMS19 in the CIA system (9, 10).

Although a previous study showed that MMS19 is not expressed in mitochondria (13), we did detect the mitochondrial Fe-S proteins succinate dehydrogenase (ubiquinone) iron-sulfur subunit (SDHB) and cytochrome bc_1 complex subunit Rieske (UQCRFS1) after MMS19, CIAO1, and MIP18 immunoprecipitation (Fig. 1, *C–E*). Purification of mitochondria did show that MMS19, CIAO1, and MIP18 are not expressed in mitochondria (Fig. 2*A*), whereas mitochondrial proteins ATP synthase subunit α, mitochondrial (ATP5A), cytochrome bc_1 complex subunit 2, mitochondrial (UQCRC2), cytochrome *c* oxidase subunit 2 (MT-CO_2), and NADH dehydrogenase (ubiquinone) 1β subcomplex subunit 8-mitochondrial (NDUFB8) were readily detected. These mitochondrial proteins were not detected in cytosolic fractions upon MMS19, CIAO1, or MIP18 IP (Fig. 2, *B* and *C*). The presence of SDHB and UQCRFS1 in IPs with cytosolic cell fractions indicates that these mitochondrial proteins are present in the cytosol. As MMS19, CIAO1, and MIP18 are not localized to mitochondria, these proteins are most likely not part of the ISC machinery.

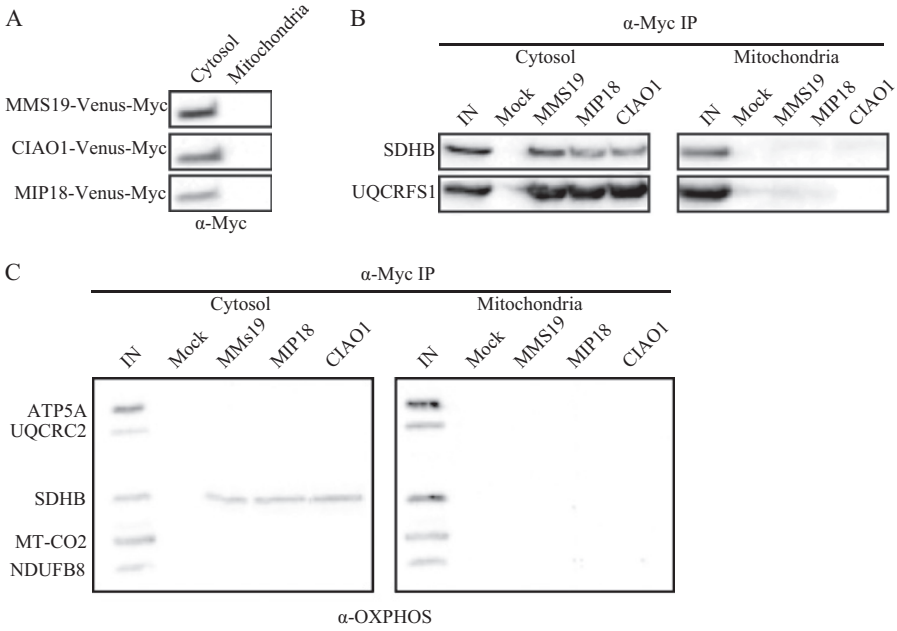

FIGURE 2. **MMS19, MIP18, and CIAO1 do not localize to mitochondria.** *A*, anti-Myc immunoblot of cytosolic and mitochondrial HEK293 fractions. *B* and *C*, Venus-Myc-tagged MMS19, CIAO1, or MIP18 was immunoprecipitated from cytosolic and mitochondrial HEK293 cell lysates. Membranes were immunoblotted with the indicated antibodies. Mock IPs were performed by incubating the wild type with anti-Myc beads. *IN*, input; *Mock*, mock-immunoprecipitated fraction; *IP*, immunoprecipitated fraction.

However, the observed interactions suggest that CIA complex protein members are capable of recognizing mitochondrial Fe-S proteins, perhaps via shared protein motifs.

MMS19 and MIP18 Interact Directly with CIAO1 and Fe-S Proteins—In determining the exact composition of the late CIA complex, we used an *in vitro* transcription and translation system to synthesize Myc-tagged MMS19, CIAO1, MIP18, and NARFL as well as FLAG-tagged CIA and Fe-S proteins. Immunoprecipitation and Western blot analysis showed that MMS19 and MIP18 interacted directly with the CIA proteins CIAO1 and NARFL but not with ANT2, CIAPIN1, or NUBP2 or with each other (Fig. 3). Furthermore, the results showed that both MMS19 and MIP18 were capable of interacting directly with the Fe-S proteins XPD, FANCJ, RTEL1, probable ATP-dependent RNA helicase DDX11 (DDX11), DNA2, MPG, A/G-specific adenine DNA glycosylase (MUTYH), SDHB, and UQCRFS1. In contrast, CIAO1 was only capable of interacting directly with MMS19, MIP18, and NARFL but not with ANT2, CIAPIN, NUBP2, or any of the Fe-S proteins. NARFL interacted with MMS19, CIAO1, and MIP18, but the results also showed it was not capable of interacting with Fe-S proteins or CIA proteins ANT2, NUBP2, and CIAPIN1. The negative control protein Poly(ADP-ribose) polymerase 1 (PARP1) did not interact with any of the proteins tested.

MIP18 Interacts with Fe-S Proteins through Their Fe-S Cluster Regions—To identify the domains necessary for interactions between MMS19, MIP18, and Fe-S proteins, different regions of the RTEL1 protein (Fig. 4*A*) were synthesized *in vitro*. The protein was divided into its ATPase/helicase domain (residues 1–746), which is a region that is highly conserved within the FANCJ-like family of helicases (14) (Fig. 4, *A* and *B*), and the C-terminal end of the protein (residues 747–1203). IP of MMS19 and MIP18 in the presence of these RTEL1 regions and

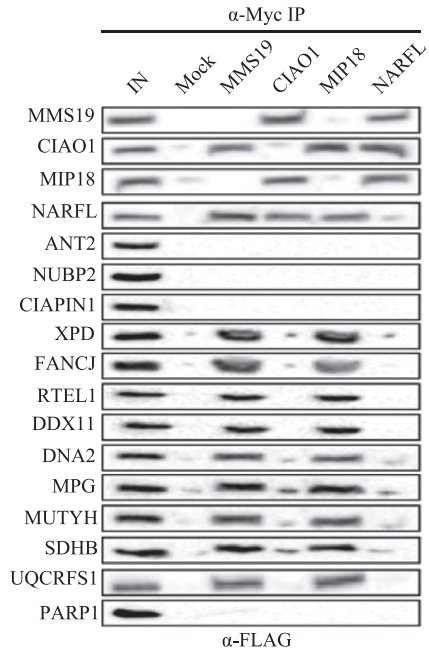

FIGURE 3. **MMS19 and MIP18 interact directly with CIAO1 and Fe-S proteins.** Myc-tagged MMS19, CIAO1, MIP18, or NARFL and FLAG-tagged CIA machinery proteins were synthesized *in vitro*. FLAG- and Myc-tagged proteins were incubated and anti-Myc immunoprecipitated. Mock IPs were performed by incubating FLAG-tagged proteins in the absence of Myc-tagged protein. *IN*, input; *Mock*, mock-immunoprecipitated fraction; *IP*, immunoprecipitated fraction. Bands that were clearly weaker than input were deemed non-specific.

subsequent Western blot analysis showed that both MMS19 and MIP18 interacted with the N-terminal RTEL1 region containing the helicase domains but not with the C-terminal end of the protein (Fig. 4*D*). To more specifically assign MMS19- and MIP18- binding regions to RTEL1, three progressively shorter regions of the helicase domain, consisting of residues 262–746,

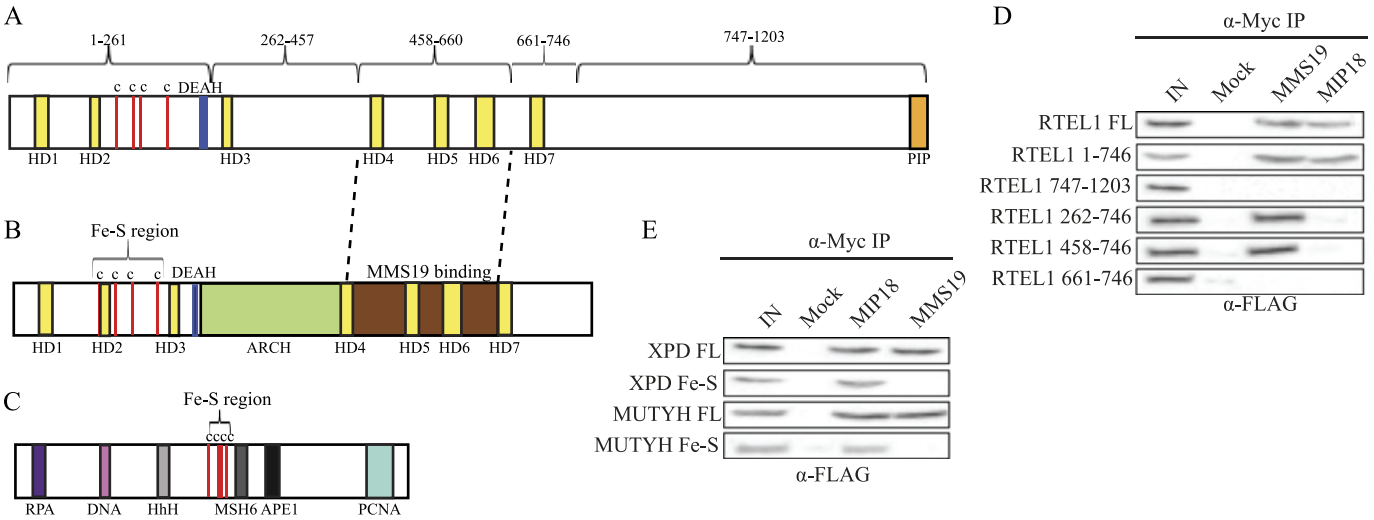

FIGURE 4. **Identification of MMS19 and MIP18-binding regions in the Fe-S protein RTEL1.** *A–C*, schematic representation of the murine RTEL1 (*A*), XPD (*B*), and MUTYH (*C*) domains. RTEL1 and XPD both contain seven helicase domains (HD1–7, *yellow*), a DEAH box (*blue*), and four cysteines necessary for the coordination of Fe-S clusters (*cccc*, *red*). RTEL1 also contains a proliferating cell nuclear antigen-interacting PIP box (*PIP*, *orange*). XPD contains an Arch domain (*ARCH*, *light green*), and the MMS19-binding region in XPD is shown in *brown*. MUTYH contains binding sites for RPA (*dark blue*), the DNA minor groove (*pink*), MSH6 (*dark gray*), APE1 (*black*), and proliferating cell nuclear antigen (*PCNA*, *light blue*). It also contains an HhH motif (*light gray*) and four Fe-S cluster coordinating cysteines (*cccc*, *red*). *D* and *E*, Myc-tagged MMS19 and MIP18 and FLAG-tagged RTEL1, XPD, and MUTYH peptides were synthesized *in vitro*. Individual FLAG-tagged proteins and Myc-tagged MMS19 or MIP18 were incubated and anti-Myc immunoprecipitated. Mock IPs were performed by incubating FLAG-tagged proteins in the absence of Myc-tagged protein. *IN*, input; *Mock*, mock-immunoprecipitated fraction; *IP*, immunoprecipitated fraction.

458–746, and 661–746, respectively, were synthesized. These three polypeptides were incubated in the presence of MMS19 or MIP18. Myc IP and Western blot analysis indicated that MMS19 was capable of interacting with RTEL1 regions 246–746 and 458–746 but not with region 661–746 (Fig. 4*D*). This indicated that the MMS19 binding site in RTEL1 lies in region 458–661, which is the region homologous to the MMS19-binding region in XPD (13) (Fig. 4, *A* and *B*). The results also showed that although MIP18 did interact with the RTEL1 helicase domain (residues 1–746), it did not interact with RTEL1 amino acids 262–746 (Fig. 4*D*). This indicates that the MIP18 binding site in RTEL1 lies at its very N-terminal region, consisting of residues 1–261. This region contains the four cysteine residues that coordinate the Fe-S cluster, and thus we hypothesized that MIP18 binds to Fe-S apoproteins in their apo-Fe-S regions.

To test this hypothesis, we synthesized polypeptides containing the Fe-S cluster coordinating cysteines from two other proteins for which the position of these cysteines are known, namely XPD and MUTYH. Polypeptides containing the four cysteines flanked by five amino acids at either side, residues 110–196 for XPD (Fig. 4*B*) and residues 257–281 for MUTYH (Fig. 4*C*), were synthesized *in vitro*, and IPs were performed in the presence of MIP18 and MMS19. Western blot analysis showed that MIP18 was capable of interacting directly with these peptides, whereas MMS19 was not (Fig. 4*E*).

MMS19 Interacts with CIAO1 and Fe-S Proteins via Different Domains—A previous study identified three MMS19 domains (A, B, and C) with distinct functions in nucleotide excision repair and transcription (Fig. 5*A*). Domains A and B are required for the role of MMS19 in transcription and nucleotide excision repair, respectively, whereas domain C is necessary for the function of MMS19 in both processes (15). Each of these domains contains one or more HEAT repeats (Fig. 5*A*), which are required for the formation of multiprotein complexes (16).

To determine whether these MMS19 regions are involved in the interactions with CIAO1 and/or Fe-S proteins, MMS19 polypeptides lacking domains A and B (MMS19ΔAB) or domain C (MMS19ΔC) were incubated in the presence of CIAO1, NARFL, XPD, and MUTYH. Myc IP and subsequent immunoblotting showed that that MMS19ΔAB retains the interaction with all four proteins, whereas MMS19ΔC no longer interacted with NARFL, XPD, and MUTYH, but it did still interact with CIAO1 (Fig. 5*B*). These results showed that MMS19 has different binding sites for CIAO1 and Fe-S proteins and that it binds Fe-S proteins through the HEAT repeats contained in its C-terminal region. The results also suggested that MMS19 binds to NARFL as an Fe-S protein and not as part of the CIA machinery.

MMS19 Binds Fe-S Cluster Donor and Acceptor Proteins Simultaneously—The previous experiments showed that MMS19 and MIP18 interact directly with CIAO1, NARFL, and Fe-S cluster proteins but not with ANT2, which was repeatedly detected in the mass spectrometry analysis (supplemental Table S2). To further determine the interactions within the complex, we designed an IP experiment with *in vitro* synthesized proteins. Myc-MMS19 was incubated with different combinations of FLAG-tagged MIP18, ANT2, CIAO1, NARFL, and XPD. Preincubation of MMS19 with XPD did not block the binding of CIAO1, suggesting that MMS19 is capable of binding CIA proteins and Fe-S proteins simultaneously (Fig. 6*A*). MIP18 could be detected after MMS19 was preincubated with XPD or with XPD and CIAO1, proving that these four proteins can form one complex.

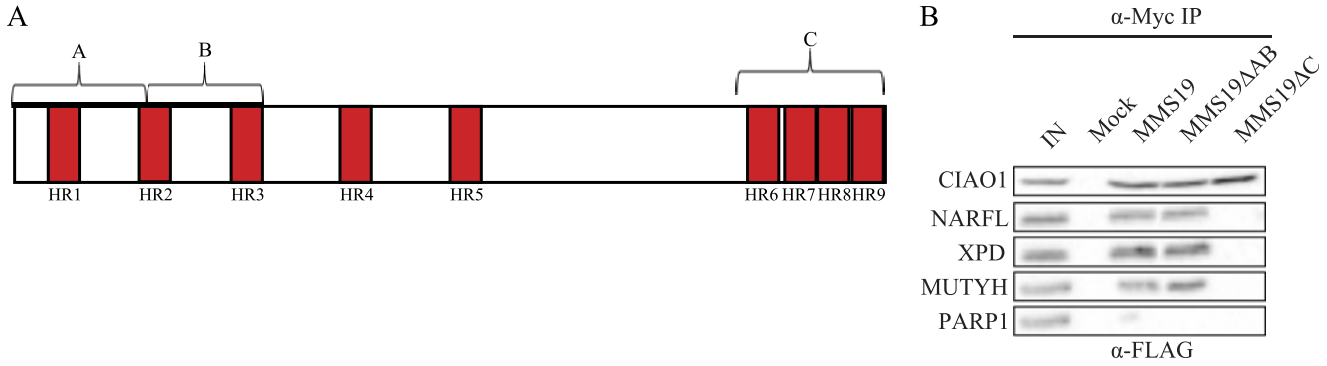

FIGURE 5. **Identification of an MMS19 domain required for the binding of Fe-S proteins.** *A*, schematic representation of the murine MMS19 domains. MMS19 contains nine HEAT repeats (*HR1–9*, *red*). *B*, Myc-tagged MMS19, MMS19ΔAB, and MMS19ΔC and FLAG-tagged CIAO1, NARFL, XPD, and MUTYH were synthesized *in vitro*. Individual FLAG-tagged proteins and Myc-tagged MMS19 or MMS19ΔC were incubated, and anti-Myc was immunoprecipitated. Mock IPs were performed by incubating FLAG-tagged proteins in the absence of Myc-tagged protein. *IN*, input; *Mock*, mock-immunoprecipitated fraction; *IP*, immunoprecipitated fraction.

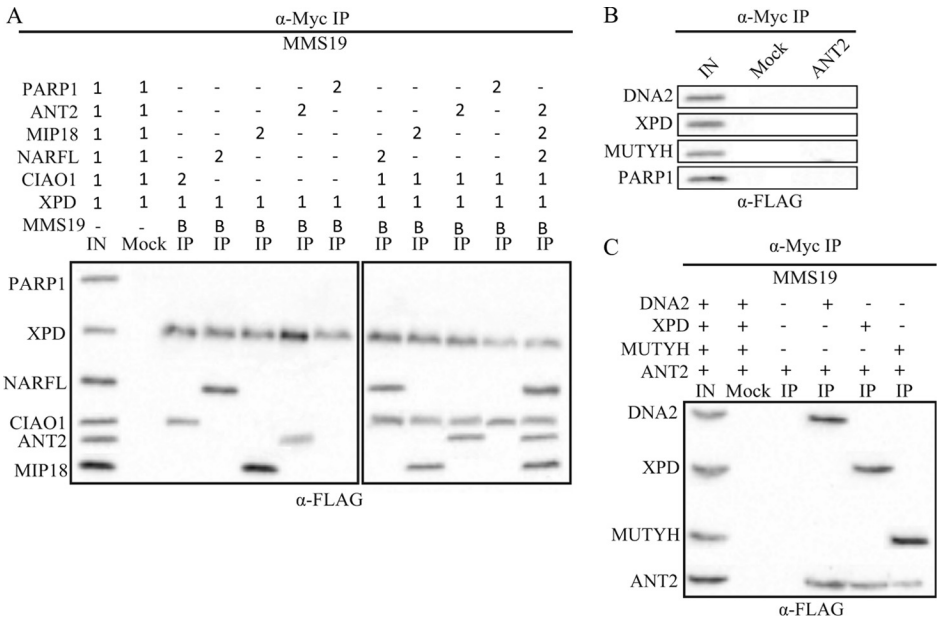

FIGURE 6. **Reconstitution of the MMS19 complex.** *A*, anti-FLAG immunoblot for FLAG-tagged CIA and Fe-S proteins interacting with Myc-tagged MMS19. Myc-tagged MMS19 and FLAG-tagged CIA and Fe-S proteins were synthesized *in vitro*. Combinations of FLAG-tagged proteins and Myc-tagged MMS19 were incubated as indicated, and anti-Myc was immunoprecipitated: *B*, bait protein; *1*, MMS19 was preincubated with this protein for the first IP; *2*, beads from the first IP were incubated in the presence of this protein for the second IP. *B*, Myc-tagged ANT2 and FLAG-tagged DNA2, XPD, MUTYH, and Parp1 were synthesized *in vitro*. Individual FLAG-tagged proteins were incubated with Myc-tagged ANT2, and anti-Myc was immunoprecipitated. *C*, Myc-tagged MMS19 and FLAG-tagged DNA2, XPD, MUTYH, and ANT2 were synthesized *in vitro*. MMS19-Myc was incubated with ANT2 alone or combined with one Fe-S protein, and Myc-was immunoprecipitated. Mock IPs were performed by incubating FLAG-tagged proteins in the absence of Myc-tagged protein. *IN*, input sample; *Mock*, mock-immunoprecipitated fraction; *IP*, immunoprecipitated fraction.

Interestingly, ANT2 was also detected after preincubation with XPD, suggesting that it bound Fe-S proteins in the presence of MMS19. To examine this possibility, Myc-tagged ANT2 was incubated in the presence of FLAG-tagged Fe-S proteins DNA2, XPD, and MUTYH. Myc IP and immunoblotting showed that ANT2 did not interact directly with Fe-S proteins *in vitro* (Fig. 6*B*). However, when FLAG-tagged ANT2 and Fe-S proteins DNA2, XPD, and MUTYH were incubated in the presence of Myc-tagged MMS19, an ANT2-MMS19-Fe-S protein complex was formed (Fig. 6*C*).

DISCUSSION

MMS19 function has been linked previously to nuclear processes like nucleotide excision repair, transcription (17, 18), DNA replication, histone modification (19), and chromosome segregation (13). Interactions among the MMS19 homolog DNA repair/transcription protein MET18/MMS19 (Met18), Cia1 (20), Nar1 (21), and the MIP18 homolog MIP18 family protein YHR122W (Yhr122w) (22) were identified previously in screens for protein complexes in budding yeast. Human MMS19 was shown to be part of the MMXD complex, which also contains CIAO1, MIP18, XPD, and ANT2 (13). Recently, MMS19 was implicated in the CIA machinery as part of a complex that includes CIAO1, MIP18 (9, 10), and NARFL (9), three known components of the CIA system (2, 23). Furthermore, MMS19 is required for cytosolic Fe-S cluster assembly of several Fe-S proteins involved in DNA metabolism (9, 10).

Here, we have further characterized the protein composition of this late acting CIA complex and the protein domains required for protein-protein interactions. We show that

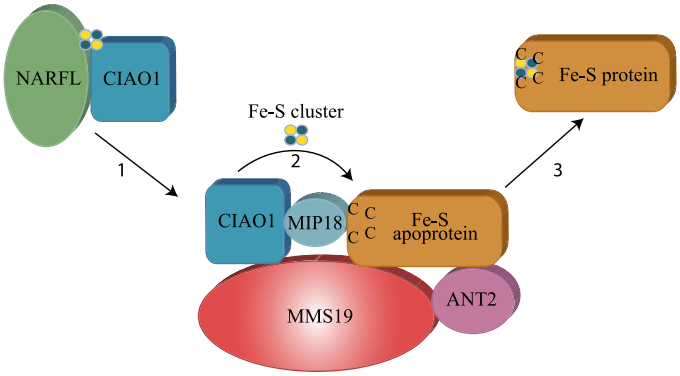

FIGURE 7. **Model for the last steps in the CIA process.** Labile Fe-S clusters are transferred to the CIAO1-NARFL complex in an earlier step. 1) CIAO1 binds directly to MMS19, which can simultaneously bind an Fe-S apoprotein. ANT2 also binds this complex, possibly in order to stabilize the interactions. 2) MIP18 interacts with both CIAO1 and the Fe-S cluster coordinating region of target Fe-S proteins (indicated by the *four Cs*, for cysteine) to facilitate the insertion of Fe-S clusters into target proteins. 3) After insertion of the Fe-S cluster, the functional Fe-S proteins dissociates from this late acting CIA complex. This model identifies MMS19 and MIP18 as components of the CIA machinery with a critical role in Fe-S protein maturation.

MMS19 interacts with the CIA component CIAO1 and Fe-S proteins simultaneously. We also show that MMS19 interacts with Fe-S target proteins through its C-terminal HEAT repeats, which have been associated previously with the formation of multiprotein complexes (16). Based on these findings, we propose that the role of MMS19 in the CIA machinery is to bridge the gap between Fe-S cluster donor and acceptor proteins.

Furthermore, we have identified the MMS19-binding region in RTEL1, which is homologous to the MMS19 binding site in XPD reported previously (13). However, no obvious homology between Fe-S proteins beyond the FANCJ-like family of helicases could be detected. This suggests that MMS19 might recognize a structural feature in Fe-S apoproteins as opposed to recognizing a stretch of specific amino acids.

A direct interaction between human GST-MIP18, purified from bacteria, and human FLAG-MMS19 and XPD-FLAG, purified from insect cells, was reported (13). However, we show here that MIP18 connects indirectly to MMS19 through interactions with CIAO1 and Fe-S proteins. MIP18 binds to the regions of Fe-S proteins that contain the four Fe-S cluster coordinating cysteines, suggesting a role for MIP18 in the actual insertion of Fe-S cluster into apoproteins.

We also show that ANT2 binds to the complex of MMS19 and Fe-S protein but not to the individual proteins. A possible role for ANT2 in the CIA system is to stabilize the interaction between MMS19 and Fe-S proteins. This also explains why ANT2 was abundant in the mass spectrometry analysis of MMS19, CIAO1, and MIP18 IP fractions, as it was likely purified along with several different Fe-S proteins.

Interestingly, we did not find NARFL in the MMS19 and RTEL1 IP-mass spectrometry analysis. *In vitro*, we did find that NARFL interacts directly with CIAO1, MMS19, and MIP18. However, our data suggest that MMS19 and MIP18 bind to NARFL because it is an Fe-S protein and not because of its role in the CIA machinery. The CIAO1-NARFL interaction is part of the CIA machinery (7), and we found no evidence that CIAO1 can interact directly with Fe-S proteins. Together, these results suggest that NARFL might only be transiently involved in the CIAO1-MMS19-MIP18 complex.

Although MMS19 and MIP18 are capable of binding directly to the mitochondrial Fe-S proteins SDHB and UQCRFS1, these proteins receive their Fe-S clusters from the ISC system, in which MMS19, CIAO1, and MIP18 are not involved. The SDHB and UQCRFS1 observed in our experiments is most likely mitochondrial contamination in the cytoplasmic cell extract, and our data suggest that they do not represent functional interactions. This is supported by the observation that depletion of human MMS19 does not reduce the activity of SDHB or mitochondrial aconitase (10).

In yeast, MMS19 deficiency leads to deficiencies in polymerase II transcription and nucleotide excision repair and increased sensitivity to methanesulfonate (MMS) and UV (17), whereas a defect in chromosome segregation has been observed in human cells (13). This pleiotropic phenotype can be explained by the newly discovered role of MMS19 in the CIA machinery, as Fe-S proteins are involved in each of these processes (9, 10). Based on our results, we propose a more detailed model for the role of both MMS19 and MIP18 in CIA (Fig. 7). In this model, MMS19 binds directly to both the Fe-S cluster donor CIAO1 and an Fe-S apoprotein into which the Fe-S cluster is to be inserted. These interactions bring the proteins into close proximity, which allows the Fe-S cluster to be transferred and inserted into the Fe-S apoprotein with the help of MIP18. ANT2 is most likely required to stabilize this complex, as it can only bind if both MMS19 and an Fe-S protein are present. After transfer of the Fe-S cluster, the functional Fe-S protein dissociates from this late CIA complex and is capable of performing its function in the cell.

In summary, we have elucidated the composition of the late acting CIA complex that contains CIAO1, MMS19, MIP18, and ANT2 and is required for the insertion of Fe-S clusters into target proteins. We have identified several direct interactions within this complex as well as protein regions required for these interactions and proposed a new model of action for this late acting CIA complex. CIA is an essential biological process, and its impairment has direct impact on the functionality of cytoplasmic and nuclear Fe-S proteins required for a wide range of cellular functions. Our findings clarify the roles of and interactions between pro-

teins within the CIA complex and its role in the crucial biological process of Fe-S protein assembly.

Acknowledgments—We thank Prof. Gerald de Haan for the use of his equipment and facilities. We are most grateful to Dr. Grace Cheng for advice and technical assistance. In addition, we thank Dr. Diana Spierings for helpful comments and critical reading of this manuscript.

REFERENCES

1. Lill, R. (2009) Function and biogenesis of iron-sulphur proteins. *Nature* **460,** 831–838
2. Lill, R., and Mühlenhoff, U. (2008) Maturation of iron-sulfur proteins in eukaryotes: mechanisms, connected processes, and diseases. *Annu. Rev. Biochem.* **77,** 669–700
3. Sharma, A. K., Pallesen, L. J., Spang, R. J., and Walden, W. E. (2010) Cytosolic iron-sulfur cluster assembly (CIA) system: factors, mechanism, and relevance to cellular iron regulation. *J. Biol. Chem.* **285,** 26745–26751
4. Hausmann, A., Aguilar Netz, D. J., Balk, J., Pierik, A. J., Mühlenhoff, U., and Lill, R. (2005) The eukaryotic P loop NTPase Nbp35: an essential component of the cytosolic and nuclear iron-sulfur protein assembly machinery. *Proc. Natl. Acad. Sci. U.S.A.* **102,** 3266–3271
5. Roy, A., Solodovnikova, N., Nicholson, T., Antholine, W., and Walden, W. E. (2003) A novel eukaryotic factor for cytosolic Fe-S cluster assembly. *EMBO J.* **22,** 4826–4835
6. Zhang, Y., Lyver, E. R., Nakamaru-Ogiso, E., Yoon, H., Amutha, B., Lee, D. W., Bi, E., Ohnishi, T., Daldal, F., Pain, D., and Dancis, A. (2008) Dre2, a conserved eukaryotic Fe/S cluster protein, functions in cytosolic Fe/S protein biogenesis. *Mol. Cell. Biol.* **28,** 5569–5582
7. Balk, J., Pierik, A. J., Netz, D. J., Mühlenhoff, U., and Lill, R. (2004) The hydrogenase-like Nar1p is essential for maturation of cytosolic and nuclear iron-sulphur proteins. *EMBO J.* **23,** 2105–2115
8. Srinivasan, V., Netz, D. J., Webert, H., Mascarenhas, J., Pierik, A. J., Michel, H., and Lill, R. (2007) Structure of the yeast WD40 domain protein Cia1, a component acting late in iron-sulfur protein biogenesis. *Structure* **15,** 1246–1257
9. Gari, K., León Ortiz, A. M., Borel, V., Flynn, H., Skehel, J. M., and Boulton, S. J. (2012) MMS19 links cytoplasmic iron-sulfur cluster assembly to DNA metabolism. *Science* **337,** 243–245
10. Stehling, O., Vashisht, A. A., Mascarenhas, J., Jonsson, Z. O., Sharma, T., Netz, D. J., Pierik, A. J., Wohlschlegel, J. A., and Lill, R. (2012) MMS19 assembles iron-sulfur proteins required for DNA metabolism and genomic integrity. *Science* **337,** 195–199
11. Uringa, E. J., Lisaingo, K., Pickett, H. A., Brind'Amour, J., Rohde, J. H., Zelensky, A., Essers, J., and Lansdorp, P. M. (2012) RTEL1 contributes to DNA replication, repair and telomere maintenance. *Mol. Biol. Cell* **23,** 2782–2792
12. Mead, C. L., Kuzyk, M. A., Moradian, A., Wilson, G. M., Holt, R. A., and Morin, G. B. (2010) Cytosolic protein interactions of the schizophrenia susceptibility gene dysbindin. *J. Neurochem.* **113,** 1491–1503
13. Ito, S., Tan, L. J., Andoh, D., Narita, T., Seki, M., Hirano, Y., Narita, K., Kuraoka, I., Hiraoka, Y., and Tanaka, K. (2010) MMXD, a TFIIH-independent XPD-MMS19 protein complex involved in chromosome segregation. *Mol. Cell* **39,** 632–640
14. Wu, Y., Suhasini, A. N., and Brosh, R. M., Jr. (2009) Welcome the family of FANCJ-like helicases to the block of genome stability maintenance proteins. *Cell. Mol. Life Sci.* **66,** 1209–1222
15. Hatfield, M. D., Reis, A. M., Obeso, D., Cook, J. R., Thompson, D. M., Rao, M., Friedberg, E. C., and Queimado, L. (2006) Identification of MMS19 domains with distinct functions in NER and transcription. *DNA Repair* **5,** 914–924
16. Andrade, M. A., and Bork, P. (1995) HEAT repeats in the Huntington's disease protein. *Nat. Genet.* **11,** 115–116
17. Lauder, S., Bankmann, M., Guzder, S. N., Sung, P., Prakash, L., and Prakash, S. (1996) Dual requirement for the yeast MMS19 gene in DNA repair and RNA polymerase II transcription. *Mol. Cell. Biol.* **16,** 6783–6793
18. Lombaerts, M., Tijsterman, M., Verhage, R. A., and Brouwer, J. (1997) *Saccharomyces cerevisiae* mms19 mutants are deficient in transcription-coupled and global nucleotide excision repair. *Nucleic Acids Res.* **25,** 3974–3979 ***9321645***
19. Li, F., Martienssen, R., and Cande, W. Z. (2011) Coordination of DNA replication and histone modification by the Rik1-Dos2 complex. *Nature* **475,** 244–248
20. Ho, Y., Gruhler, A., Heilbut, A., Bader, G. D., Moore, L., Adams, S. L., Millar, A., Taylor, P., Bennett, K., Boutilier, K., Yang, L., Wolting, C., Donaldson, I., Schandorff, S., Shewnarane, J., Vo, M., Taggart, J., Goudreault, M., Muskat, B., Alfarano, C., Dewar, D., Lin, Z., Michalickova, K., Willems, A. R., Sassi, H., Nielsen, P. A., Rasmussen, K. J., Andersen, J. R., Johansen, L. E., Hansen, L. H., Jespersen, H., Podtelejnikov, A., Nielsen, E., Crawford, J., Poulsen, V., Sørensen, B. D., Matthiesen, J., Hendrickson, R. C., Gleeson, F., Pawson, T., Moran, M. F., Durocher, D., Mann, M., Hogue, C. W., Figeys, D., and Tyers, M. (2002) Systematic identification of protein complexes in *Saccharomyces cerevisiae* by mass spectrometry. *Nature* **415,** 180–183
21. Gavin, A. C., Aloy, P., Grandi, P., Krause, R., Boesche, M., Marzioch, M., Rau, C., Jensen, L. J., Bastuck, S., Dümpelfeld, B., Edelmann, A., Heurtier, M. A., Hoffman, V., Hoefert, C., Klein, K., Hudak, M., Michon, A. M., Schelder, M., Schirle, M., Remor, M., Rudi, T., Hooper, S., Bauer, A., Bouwmeester, T., Casari, G., Drewes, G., Neubauer, G., Rick, J. M., Kuster, B., Bork, P., Russell, R. B., and Superti-Furga, G. (2006) Proteome survey reveals modularity of the yeast cell machinery. *Nature* **440,** 631–636
22. Jin, F., Hazbun, T., Michaud, G. A., Salcius, M., Predki, P. F., Fields, S., and Huang, J. (2006) A pooling-deconvolution strategy for biological network elucidation. *Nat. Methods* **3,** 183–189
23. Weerapana, E., Wang, C., Simon, G. M., Richter, F., Khare, S., Dillon, M. B., Bachovchin, D. A., Mowen, K., Baker, D., and Cravatt, B. F. (2010) Quantitative reactivity profiling predicts functional cysteines in proteomes. *Nature* **468,** 790–795